Published in final edited form as:

Mult Scler. 2020 July ; 26(8): 987–992. doi:10.1177/1352458519828297.

White-matter-nulled MPRAGE at 7T reveals thalamic lesions and atrophy of specific thalamic nuclei in multiple sclerosis

Vincent Planche[1,2,3,*], **Jason H. Su**[4,*], **Sandy Mournet**[3], **Manojkumar Saranathan**[5], **Vincent Dousset**[2,3,6], **May Han**[7], **Brian K. Rutt**[8,†], **Thomas Tourdias**[2,3,6,†]

[1]Institut des Maladies Neurodégénératives, CNRS UMR 5293, F-33000 Bordeaux, France

[2]Univ. Bordeaux, F-33000 Bordeaux, France

[3]CHU de Bordeaux, F-33000 Bordeaux, France

[4]Electrical Engineering, Stanford University, Stanford, CA, USA

[5]Medical Imaging, University of Arizona, Tucson, AZ, USA

[6]INSERM U1215, Neurocentre Magendie, F-33000 Bordeaux, France

[7]Departments of Neurology, Stanford University School of Medicine, Palo Alto, CA, USA

[8]Radiology, Stanford University, Stanford, CA, USA

Abstract

Background: Investigating the degeneration of specific thalamic nuclei in multiple sclerosis (MS) remains challenging.

Methods: White-matter-nulled (WMn) MPRAGE, MP-FLAIR and standard T1-weighted MRI were performed on MS patients (n=15) and matched controls (n=12). Thalamic lesions were counted in individual sequences and lesion contrast-to-noise ratio (CNR) was measured. Volumes of 12 thalamic nuclei were measured using an automatic segmentation pipeline specifically developed for WMn-MPRAGE.

Results: WMn-MPRAGE showed more thalamic MS lesions (n=35 in 9/15 patients) than MP-FLAIR (n=25) and standard T1 (n=23), which was associated with significant improvement of CNR ($p<0.0001$). MS patients had whole thalamus atrophy ($p=0.003$) with lower volumes found for the anteroventral ($p<0.001$), the pulvinar ($p<0.0001$) and the habenular ($p=0.004$) nuclei.

Conclusions: WMn-MPRAGE and automatic thalamic segmentation can highlight thalamic MS lesions and measure patterns of focal thalamic atrophy.

Keywords

Thalamic nuclei; multiple sclerosis; multi-atlas segmentation; white matter nulled MPRAGE; ultra-high field MRI

Correspondence should be addressed to Vincent Planche, CNRS UMR 5293, Institut des Maladies neurodégénératives, 146 rue Léo Saignat, 33000 Bordeaux, France, vincent.planche@u-bordeaux.fr, Phone: +33 (0)5 56 79 56 79, Fax: +33 (0)5 56 79 56 39.

*Both authors contributed equally to this work

†Share seniority

Introduction

Thalamic pathology in multiple sclerosis (MS) has been correlated with a wide range of symptoms (1). This highlights the complexity of the thalamus as a non-unitary entity composed of distinct nuclei that are very different in their connectivity, morphological and functional profiles (2). Rather than studying the thalamus as a whole, more insight could be gained by studying thalamic nuclei separately.

To develop such an analysis of individual thalamic nuclei, we used a white-matter-nulled (WMn) MPRAGE sequence at ultra-high field (7T) to produce high intrinsic contrast between adjacent thalamic nuclei (3). The high intra-thalamic contrast in WMn-MPRAGE allows the direct visualization of individual histologically-related thalamic nuclei and the measurement of their volumes (3). We believe that this approach confers advantage over previously proposed methods for investigating thalamic subregions such as deformation-based or vertex-wise shape analyses (4), probabilistic atlases (5) or connectivity-derived parcellation of the thalamus (6). Furthermore, we hypothesized that the high intrinsic contrast of the WMn-MPRAGE sequence would also be useful for highlighting thalamic MS lesions that usually go unnoticed on conventional imaging.

Materials and Methods

Participants

Fifteen patients with MS were prospectively recruited at the Stanford MS Center. According to 2005 McDonald's criteria, 13 patients had relapsing-remitting MS, while 2 patients had secondary-progressive MS. We recruited 12 healthy control subjects tightly matched for age and sex to the MS patients, who were free of neurologic, psychiatric, or systemic diseases, and of drug or alcohol abuse. Informed consent was obtained from all patients and volunteers, and the study was approved by the institutional review board.

MRI acquisition and post-processing technics

Patients and controls were scanned on a 7T scanner (Discovery MR950; GE Healthcare). We collected conventional 3D-T1 weighted MPRAGE, MP-FLAIR and the WMn-MPRAGE. Acquisition parameters are described in Supplementary Material.

Manual segmentation of individual thalamic nuclei on WMn-MPRAGE images was accomplished by an expert neuroradiologist and was found to produce boundaries that correspond well with known anatomical structures from the histological Morel atlas (3); however this was a tedious process requiring several hours per case. We therefore used 20 of these cases to create a library of "priors" that was used to train a multi-atlas label fusion segmentation algorithm (8). We named this automatic segmentation pipeline "THOMAS" for THalamus-Optimized-Multi-Atlas-Segmentation; the pipeline is described in detail in Supplementary Material. THOMAS generates masks of the whole thalamus and 12 individual thalamic nuclei (Fig. 1A and Suppl. Fig. 1)

Thalamic lesions, defined as hyperintense on MP-FLAIR and WMn-MPRAGE and hypointense on standard MPRAGE, were demarcated in a blinded manner. Contrast-to-noise

ratio (CNR) between thalamic lesions and the adjacent thalamic parenchyma was calculated for a subset of the largest lesions (n=13). Finally, T2-lesion load was computed from FLAIR images and normalized brain volume was calculated from standard T1 images using VolBrain (http://volbrain.upv.es).

Statistical analyses

We compared demographic and general MRI characteristics between healthy controls and patients using Fisher's exact test for categorical variables, and the Mann–Whitney test for ordinal variables. CNR was compared between sequences by using ANOVA and Tukey-Kramer post-hoc comparisons. We used multiple linear regressions (MLR) to test the association between the volumes of thalamic nuclei and the diagnostic category (patient or control) adjusted for standard confounders (age, sex and intracranial cavity volume). Bonferroni correction was used in MLR analyses (13 comparisons for 12 nuclei plus whole thalamus). Correlations between thalamic volumes, T2-lesion load or normalized brain volume were tested using Pearson coefficients.

Results

Demographic and general MRI features of participants:

Mean disease duration was 7.9±7.2 years and all patients but one were undergoing disease-modifying therapy at the time of the study (Glatiramer acetate, IFN beta, Natalizumab). There were no significant differences in age or sex between patients and healthy volunteers (mean ages 39.8±9.8 and 40.0±8.0 years and female/male ratios 9/6 and 7/5, respectively). Patients showed a median T2-lesion load of 1842 mm^3 (range, 154–17564mm^3) and a significant decrease of normalized brain volume compared to controls (median variation of −8.4%, p=0.0061).

Thalamic lesions:

9/15 patients showed at least one thalamic lesion (35 lesions in total) on the WMn-MPRAGE sequence. The median number of lesions *per* patient was 2 [range: 0 – 14] with a median volume of 22.7mm^3 [range: 0 – 482.8mm^3]. By coupling the lesion delineation with the nuclei segmentation (Fig.1A), we found that most of the lesions were located within nuclei adjacent to the third ventricle (pulvinar, mediodorsal, ventral-anterior and the adjacent anteroventral nuclei in 79% of the cases) and appeared with band-like shapes lining the ependymal surface (54.5% of the cases). The blinded reading of standard T1 and MP-FLAIR counted fewer lesions compared to WMn-MPRAGE (n=23 and 25 total lesions respectively) and in several cases, thalamic lesions were mainly seen on the WMn-MPRAGE sequence while they were barely visible on MP-FLAIR or standard T1-weighted images (Fig.1C; other examples can be seen in Suppl. Fig.2). In line with this lesion counting, quantification of lesion-CNR was significantly higher with WMn-MPRAGE compared to conventional sequences (p<0.0001, Fig.1B) with a mean increase of 238% compared to standard T1 and of 381% compared to MP-FLAIR.

Thalamic nuclei volumes:

Thalamic nuclei were automatically segmented on WMn-MPRAGE using the THOMAS algorithm. During careful visual inspection of the automatic segmentation it was found that no significant manual editing had to be done (R^2=0.99, p<0.0001 between raw segmentations and raw + manual editing segmentations) even for patients presenting with thalamic lesions. The boundaries automatically defined were observed in expected positions along thin hypointense bands surrounding and separating adjacent nuclei or at edges defined by signal change (Fig.1A and Suppl. Fig.1).

When compared to matched healthy controls, patients with MS showed a significant decrease in whole thalamus volume (p=0.003) (Fig.2). The nucleus-by-nucleus analysis showed that such global atrophy was driven by selective volume loss (Fig.2): significant reductions in volumes were found for the anteroventral (p<0.001), the pulvinar (p<0.0001) and the habenular (p=0.004) nuclei. The volumes of the largest structures (whole thalamus and Pul) were negatively correlated to T2-lesion load (r=−0.56 and r=−0.67 respectively, p<0.03).

Discussion

In this study, we demonstrated that the WMn-MPRAGE sequence highlights individual thalamic MS lesions with higher contrast and detectability compared to conventional sequences. Secondly, we were able to measure a specific pattern of thalamic nuclear atrophy. We report that both lesions and nuclear atrophy occur predominately adjacent to the third ventricle.

While thalamic lesions have been frequently reported in post-mortem neuropathological studies (1), their *in vivo* characterization using MRI is still limited. A few reports have taken advantage of the 7T field strength to generate increased signal-to-noise ratio and resolution, and have reported the *in vivo* detection of thalamic lesions in MS, using FLAIR or T2* sequences (9, 10). Our findings corroborate these previous works by observing that thalamic lesions were frequent in relapsing-remitting and progressive MS (>50% of patients) and were most frequently found in periventricular areas. Thanks to the unique combination of lesion detection and automatic segmentation of nuclei from the same sequence, we were able to conclude that lesions were mainly located within the pulvinar, mediodorsal, ventral-anterior and anteroventral nuclei. Interestingly, our results suggest that the WMn-MPRAGE sequence is more sensitive for the detection of thalamic lesions than more conventional MP-FLAIR or T1-weighted sequences, as more lesions were counted during blinded reading, probably as a result of the significant increase in CNR. However, we acknowledge that while no lesions were found in control subjects, there is no gold standard to ascertain that the thalamic lesions detected in the MS patients are true positives.

In addition to improving thalamic lesion detection, the WMn-MPRAGE sequence produces high enough contrast to allow delineation of individual thalamic nuclei. The contrast generated is much higher than with conventional T1-weighted imaging, obviating the need for complicated shape models and enabling accurate label fusion and transfer learning from priors that we embedded within the automatic ‘THOMAS” pipeline. Furthermore, the nuclei

delineated by the WMn-MPRAGE sequence correspond well with the established Morel histological atlas (3), in contrast to other popular methods such as DTI-based segmentation; the latter typically provides only 5–6 clusters and suffers from the image distortion and limited spatial resolution inherent to DTI (11).

One of the main findings of the present study is the demonstration of differential vulnerability of specific thalamic nuclei in MS. The nuclei that we found to be significantly affected are adjacent to the ventricles in the anterior (anteroventral), medial (habenular) and posterior (pulvinar) groups. Interestingly, nuclei of the lateral group (which are farther from the ventricles) were spared; these findings argue for a CSF-driven process in which CSF-mediated factors and immune cells penetrate the thalamus. A similar mechanism has recently been proposed to explain the differential vulnerability of hippocampal subfields in MS (12). However, such a selective pattern of thalamic nuclei atrophy warrants further investigation in larger samples of patients and in different MS populations. It will also be interesting to investigate in future studies the clinical relevance of specific thalamic nuclei atrophy. We are currently investigating whether 3T WMn-MPRAGE data (13) can be used to automatically segment thalamic nuclei using the THOMAS algorithm to allow broader clinical application.

Supplementary Material

Refer to Web version on PubMed Central for supplementary material.

Acknowledgments:

We thank Bruno Brochet, Aurélie Ruet, Ismail Koubiyr and Mathilde Deloire for helpful discussions.

Conflicts of Interest and Source of Funding

This study was supported by the ARSEP Fondation. The work was further supported by public grants from the French Agence Nationale de la Recherche within the context of the Investments for the Future programme referenced ANR-10-LABX-57 named TRAIL (project GM-COG) and ANR-10-LABX-43 named BRAIN (Project MEMO-MS). The sponsors did not participate in any aspect of the design or performance of the study, including data collection, management, analysis and interpretation or the preparation, review and approval of the manuscript. JS, MS and BR were supported by grants from the National Institutes of Health (US): NIH P41 EB015891, and by a grant from GE Healthcare.

References

1. Minagar A, Barnett MH, Benedict RH, Pelletier D, Pirko I, Sahraian MA, et al. The thalamus and multiple sclerosis: Modern views on pathologic, imaging, and clinical aspects. Neurology 2013;80(2):210–9. [PubMed: 23296131]
2. Kipp M, Wagenknecht N, Beyer C, Samer S, Wuerfel J, Nikoubashman O. Thalamus pathology in multiple sclerosis: from biology to clinical application. Cell Mol Life Sci 2015;72(6):1127–47. [PubMed: 25417212]
3. Tourdias T, Saranathan M, Levesque IR, Su J, Rutt BK. Visualization of intra-thalamic nuclei with optimized white-matter-nulled MPRAGE at 7T. Neuroimage 2014;84:534–45. [PubMed: 24018302]
4. Bergsland N, Zivadinov R, Dwyer MG, Weinstock-Guttman B, Benedict RH. Localized atrophy of the thalamus and slowed cognitive processing speed in MS patients. Mult Scler 2016;22(10):1327–36.. [PubMed: 26541795]
5. Liu Y, Duan Y, Huang J, Ren Z, Ye J, Dong H, et al. Multimodal Quantitative MR Imaging of the Thalamus in Multiple Sclerosis and Neuromyelitis Optica. Radiology 2015:142786.

6. Bisecco A, Rocca MA, Pagani E, Mancini L, Enzinger C, Gallo A, et al. Connectivity-based parcellation of the thalamus in multiple sclerosis and its implications for cognitive impairment: A multicenter study. Hum Brain Mapp 2015;36(7):2809–25. [PubMed: 25873194]
7. Saranathan M, Tourdias T, Kerr AB, Bernstein JD, Kerchner GA, Han MH, et al. Optimization of magnetization-prepared 3-dimensional fluid attenuated inversion recovery imaging for lesion detection at 7 T. Invest Radiol 2014;49(5):290–8. [PubMed: 24566291]
8. Rohlfing T, Brandt R, Menzel R, Maurer CR Jr. Evaluation of atlas selection strategies for atlas-based image segmentation with application to confocal microscopy images of bee brains. Neuroimage 2004;21(4):1428–42. [PubMed: 15050568]
9. Harrison DM, Oh J, Roy S, Wood ET, Whetstone A, Seigo MA, et al. Thalamic lesions in multiple sclerosis by 7T MRI: Clinical implications and relationship to cortical pathology. Mult Scler 2015;21(9):1139–50. [PubMed: 25583851]
10. Louapre C, Govindarajan ST, Gianni C, Madigan N, Sloane JA, Treaba CA, et al. Heterogeneous pathological processes account for thalamic degeneration in multiple sclerosis: Insights from 7 T imaging. Mult Scler 2017:1352458517726382.
11. Battistella G, Najdenovska E, Maeder P, Ghazaleh N, Daducci A, Thiran JP, et al. Robust thalamic nuclei segmentation method based on local diffusion magnetic resonance properties. Brain Struct Funct 2017;222(5):2203–16. [PubMed: 27888345]
12. Planche V, Koubiyr I, Romero JE, Manjon JV, Coupe P, Deloire M, et al. Regional hippocampal vulnerability in early multiple sclerosis: Dynamic pathological spreading from dentate gyrus to CA1. Hum Brain Mapp 2018;39(4):1814–24. [PubMed: 29331060]
13. Saranathan M, Tourdias T, Bayram E, Ghanouni P, Rutt BK. Optimization of white-matter-nulled magnetization prepared rapid gradient echo (MP-RAGE) imaging. Magn Reson Med 2015;73(5):1786–94. [PubMed: 24889754]

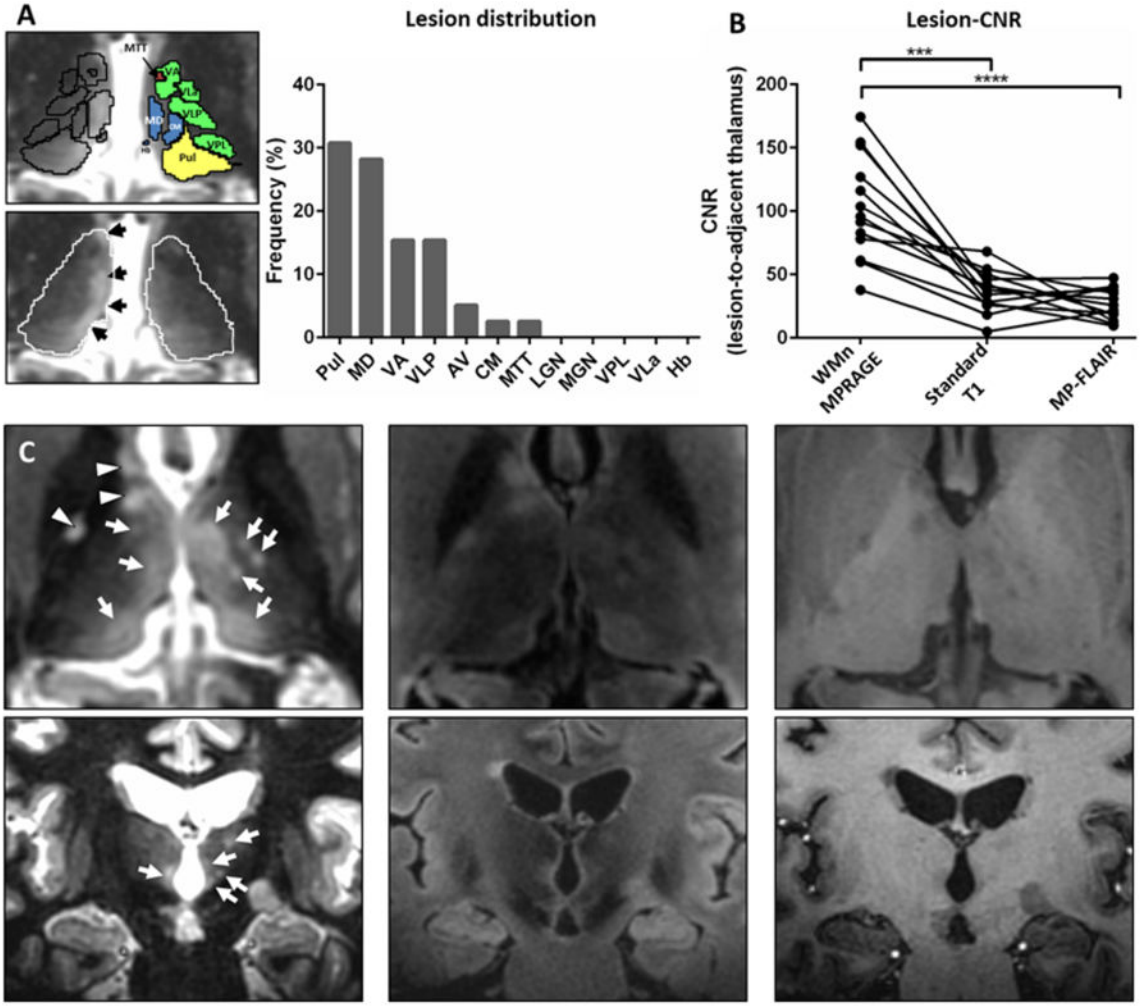

Figure 1: WMn-MPRAGE and detection of thalamic lesions

(A) The THOMAS pipeline generates masks of the whole thalamus and 12 individual thalamic nuclei: *(i)* from the anterior group (red), the anteroventral nucleus (AV) and the mamillothalamic tract (MTT); *(ii)* from the medial group (blue): the mediodorsal nucleus (MD), the center median nucleus (CM) and the habenular nucleus (Hb); *(iii)* from the posterior group (yellow): the pulvinar (Pul), the lateral geniculate nucleus (LGN) and the medial geniculate nucleus (MGN); *(iv)* from the lateral group (green): the ventral anterior nucleus (VA), the ventral lateral anterior nucleus (VLa), the ventral lateral posterior nucleus (VLP) and the ventral posterior lateral nucleus (VPL). Here, one illustrative example is shown with lesions indicated with arrows that appeared as bands lining along the ependymal surface and that are located within Pul, MD and VA based on overlapped with segmentation. The bar plot shows the distribution of the 35 MS lesions seen on WMn-MPRAGE within the 12 automatically segmented thalamic nuclei. Most lesions were detected within nuclei adjacent to the third ventricle (namely Pul, MD, VA and the adjacent AV nuclei).

(B) shows contrast-to-noise ratio (CNR) between thalamic lesion and adjacent parenchyma as measured in the subset of the 13 largest thalamic lesions seen on WMn-MPRAGE, standard T1 and MP-FLAIR. CNR was defined as $(S_{lesion}-S_{adjacent})/SD_{background}$ for

WMn-MPRAGE and MP-FLAIR because lesions appeared hyperintense and as ($S_{adjacent}$ -S_{lesion})/$SD_{background}$ for standard T1 because lesions appeared hypointense. $SD_{background}$ is the standard deviation in a region of interest placed identically in air to minimize errors due to spatially varying noise characteristics. *** and **** indicates $p<0.001$ and $p<0.0001$ (ANOVA and Tukey-Kramer post-hoc comparisons).

(C) shows respectively WMn-MPRAGE, MP-FLAIR and standard T1 MPRAGE , in axial (upper panel) and coronal (lower panel) from two different patients. While white matter lesions and adjacent gray-to-white matter lesions are well seen with the three sequences within the internal capsule (arrowheads), several thalamic lesions (arrows) are better seen and mainly identified on the WMn-MPRAGE. These thalamic lesions are either ovoid or more diffuse along the surface of the ventricle.

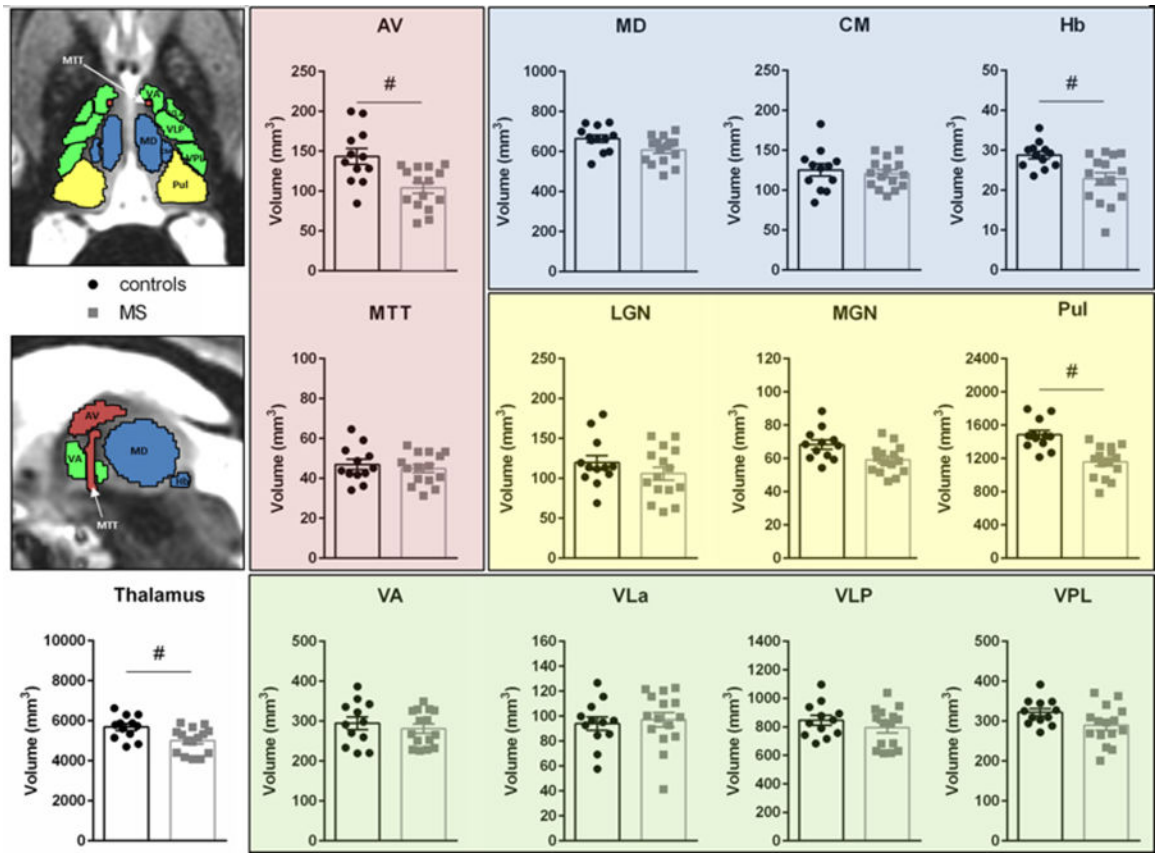

Figure 2: WMn-MPRAGE and quantification of thalamic nuclei volumes

Comparison of the volumes of thalamic nuclei between healthy controls and persons with MS. The volumes of the whole thalamus and 12 individual thalamic nuclei were measured. Axial and sagittal images illustrate the location of the nuclei whose abbreviation and color-code are as described in Figure 1 (nuclei from the medial group in blue, nuclei from the anterior group in red, nuclei from the posterior group in yellow and nuclei from the lateral group in green). # indicates $p < 0.004$ comparison between MS and control groups adjusted on age, sex and intracranial cavity volume with multiple linear regression (Bonferroni threshold).